DEUTSCHES ELEKTRONEN – SYNCHROTRON

DESY 91-104
TUM-T31-19/91
October 1991

Higgs Radiation off Top Quarks in High-Energy e^+e^- Colliders

A. Djouadi

Deutsches Elektronen-Synchrotron DESY, Hamburg

and

Institut für Theoretische Physik, RWTH Aachen

J. Kalinowski

Fakultät für Physik, Technische Universität München

P. M. Zerwas

Deutsches Elektronen-Synchrotron DESY, Hamburg

ISSN 0418-9833

NOTKESTRASSE 85 · D-2000 HAMBURG 52

DESY 91-104
TUM-T31-19/91
October 1991

ISSN 0418-9833

Higgs Radiation off Top Quarks in High–Energy e^+e^- Colliders*

A. Djouadi[1,2], J. Kalinowski[3†] and P. M. Zerwas[1]

[1] Deutsches Elektronen–Synchrotron DESY, D-2000 Hamburg 52, FRG
[2] Inst. Theor. Physik, RWTH Aachen, D-5100 Aachen, FRG
[3] Physik-Dept., TU München, D-8046 Garching/München, FRG

Abstract

Higgs particles can be radiated off heavy top quarks which will be produced copiously in high energy e^+e^- colliders. This process can be used to measure the Higgs–top quark coupling. We present the cross section for the production of Higgs bosons in the Standard Model. In addition we have studied the production of neutral and charged Higgs particles in association with heavy fermions in the Minimal Supersymmetric Standard Model.

*Supported in part by Deutsche Forschungsgemeinschaft DFG and the German Bundesministerium für Forschung und Technologie under contract 06 TM 761.
†On leave from Institute for Theoretical Physics, University of Warsaw, 00681 Warsaw, Poland.

1 Introduction

The Higgs mechanism [1] is one of the key points in the theory of the electroweak interactions[2]. The fundamental particles acquire masses through the interaction with the ground state Higgs field. As a result, the characteristic scale for the coupling of the physical Higgs boson to fermions and gauge bosons is set by the masses of these particles. This is a necessary requirement to unitarize the theory of the electroweak interactions [3]. The fundamental nature of the generation of particle masses demands this picture to be scrutinized experimentally in all facets. If the Higgs particle has been found - *conditio sine qua non* - its properties must be measured, in particular the couplings to the other fundamental particles which are uniquely fixed by the Higgs mechanism.

Various combinations of Higgs coupling constants can be determined by measurements of production cross sections, decay widths and branching ratios of this particle. The Higgs couplings to the gauge bosons W, Z are measured in the bremsstrahl processes $Z \to ZH$ [4] and the fusion processes $WW, ZZ \to H$ [5]. For sufficiently large Higgs masses the widths $\Gamma(H \to ZZ, WW)$ can be determined experimentally. Couplings to fermions are not so easily accessible. For light ($M_H \leq M_W$) and intermediate mass Higgs bosons ($M_W \leq M_H \leq 2M_W$), the width is so narrow that it cannot be resolved experimentally. The branching ratios in τ leptons and, eventually, charmed particles nevertheless reveal the couplings of these particles relative to the b–quark coupling which is predicted to provide the dominant decay mode [6]. In the upper part of the intermediate mass range, the branching ratios $BR(H \to WW^*, ZZ^*)$ can be measured [one gauge boson being virtual] so that only in this case the absolute values of the b, c, τ couplings can be derived in conjunction with the production cross sections.

The decay widths of $H \to \gamma\gamma/gg$ and the fusion mechanisms $\gamma\gamma, gg \to H$ are built–up (partly) by top quark loops with the amplitude being proportional to the Higgs–top quark coupling [7]. However, these vertices may also be affected by loops of heavy particles beyond the Standard Model so that more direct tests of the Higgs–top coupling are mandatory. For heavy Higgs bosons which can decay into $t\bar{t}$ pairs, the Yukawa $t\bar{t}H$ coupling can be measured in the process $e^+e^- \to HZ \to t\bar{t}Z$ albeit with small rates [8].

A direct way to determine the Yukawa coupling of the intermediate mass Higgs boson to the top quark in the Standard Model ($\mathcal{SM}$) is provided by the process

$$e^+e^- \longrightarrow t\bar{t}H \tag{1}$$

in high energy e^+e^- annihilation, Fig.1a. This reaction was discussed earlier in the literature as a possible source of Higgs particles at low energies where only the photon exchange diagrams need to be taken into account [9]. At high energies the Z exchange diagrams lead to an axial–vector contribution different from the vectorial γ amplitude. An additional contribution comes from Higgs bremsstrahlung off the Z boson which will however prove to be of minor importance so that the Higgs–top coupling can still be measured directly in this process. [In hadron colliders Higgs bremsstrahlung off top quarks, $gg \to t\bar{t}H$, may provide a mechanism for searching Higgs bosons in the lower part of the intermediate mass range in $l\gamma\gamma$ events [10] if the background and experimental resolution problems can be solved.]

In theories beyond the $\mathcal{SM}$ the structure of the Higgs sector is more complicated in general. As an attractive example we shall discuss in detail the Minimal Supersymmetric Standard Model ($\mathcal{MSSM}$). This model incorporates two SU(2) Higgs doublets, leading to five physical Higgs bosons: two neutral scalars h^0, H^0, one neutral pseudo-scalar A^0, plus a pair of charged Higgs particles $H^\pm$ with a mixture of scalar and pseudo-scalar couplings to fermions. [We shall distinguish SUSY Higgs particles by their charge assignments $(h^0, H^0, A^0, H^\pm)$ from the $\mathcal{SM}$ Higgs particle H.] The couplings depend on the parameter tgβ, the ratio between the vacuum expectation values of the Higgs fields which generate the masses for up-type and down-type fermions, respectively. This parameter is generally assumed to be in the range $1 \leq \mathrm{tg}\beta \leq m_t/m_b$. For large tg$\beta$ the couplings to down-type particles are enhanced over the couplings to the up-type particles.

The mechanisms that contribute to the production of neutral $\mathcal{MSSM}$ Higgs bosons in association with heavy fermions f,

$$e^+e^- \longrightarrow f\bar{f}h^0\ ,\ f\bar{f}H^0\ ,\ f\bar{f}A^0 \tag{2}$$

are shown in Figs.1b/c. Besides bremsstrahlung off the fermion and Z-boson lines, the pair production of a real and virtual scalar plus pseudo-scalar Higgs boson leads to $f\bar{f}$ + Higgs final states. If top quarks can decay into charged Higgs bosons, $t \to bH^+$ for $M_{H^\pm} \leq m_t - m_b$, the branching ratio relative to the generally dominating W-boson decay mode allows us to determine the coupling of the charged Higgs to the scalar (t,b) current. In this mass range the charged Higgs boson decays preferentially into $\tau\nu_\tau$ pairs. For $M_{H^\pm} \geq m_t + m_b$, on the other hand, the $H^\pm$ decay width and the branching ratios can be utilized. For the mass window inbetween, the radiation process

$$e^+e^- \longrightarrow t\bar{b}H^- \tag{3}$$

provides the only way to determine the $t\bar{b}H^-$ coupling, Fig.1d.

The processes under discussion are of higher order in the electroweak coupling and involve three heavy particles in the final state. As a result, they are similarly rare as Z-boson radiation in $e^+e^- \to t\bar{t}Z$ [8]. For a linear e^+e^- collider with a total c.m. energy $\sqrt{s} = 500$ GeV and a luminosity of $\mathcal{L} = 2 \times 10^{33}$ cm^{-2}s^{-1}, the $\mathcal{SM}$ reaction $e^+e^- \to t\bar{t}H$ could be measurable up to a Higgs mass of ~ 120 GeV for a top mass below ~ 150 GeV [11]. The same holds true for the light and the heavy neutral $\mathcal{CP}$-even scalar bosons in the $\mathcal{MSSM}$ for moderate values of tgβ. The $\mathcal{CP}$-odd Higgs

boson does not seem accessible unless the value of tgβ is either exceptionally small or large. For the $\mathcal{CP}$-even Higgs bosons the small radiation rate is – at least partially – balanced by the spectacular signal

$$e^+e^- \longrightarrow t\bar{t}H \longrightarrow WWbbbb \tag{4}$$

with two W's and four b quarks in the final state. Since these rare events will only be searched for after the discovery of the Higgs boson, backgrounds can strongly be reduced by exploiting the W, t and H mass constraints.

The present work extends previous studies in which the $\mathcal{SM}$ model Higgs was studied at low energies [9]; $\mathcal{CP}$-even [12,13,14], $\mathcal{CP}$-odd neutral [14] and charged Higgs radiation [12,14,15] off fermions in general two-Higgs doublet models was investigated earlier in Z decays.

2 Standard Model

Since all fermion and Higgs masses in the final state must be kept non-zero, the cross section for the $\mathcal{SM}$ process $e^+e^- \to f\bar{f}H$ is quite involved. The basic Higgs couplings are given by the Yukawa coupling [16]

$$\frac{g_{ffH}^2}{4\pi} = \frac{\sqrt{2}G_F}{4\pi}m_f^2 \tag{5}$$

and the Higgs coupling to the Z boson which for our purpose is defined most conveniently by

$$\frac{g_{ZZH}^2}{4\pi} = \frac{\sqrt{2}G_F}{4\pi}M_Z^2 \tag{6}$$

where $s_W^2 = 1 - c_W^2 = \sin^2\theta_W = 0.23$; we choose $\alpha \simeq 1/127$ for the value of the running electromagnetic coupling constant. Let us define Q_f to be the electric charge and N_c the number of quark colors, $\hat{a}_f$ and $\hat{v}_f$ the axial and vectorial Z charges of the fermion f, respectively, normalized as

$$\hat{a}_f = \frac{2I_{3L}^f}{4c_Ws_W}\ , \qquad \hat{v}_f = \frac{2I_{3L}^f - 4Q_fs_W^2}{4c_Ws_W}$$

with $I_{3L}^f = \pm 1/2$ being the weak isospin of the left-handed fermions. Evaluating the diagrams (1a), the Dalitz plot density for $e^+e^- \to f\bar{f}H$ may be written as

$$\begin{aligned}\frac{d\sigma(e^+e^- \to f\bar{f}H)}{dx_1dx_2} = N_c\frac{\sigma_0}{4\pi}\Bigg\{ &\left[Q_e^2Q_f^2 + \frac{2Q_eQ_f\hat{v}_e\hat{v}_f}{1 - M_Z^2/s} + \frac{(\hat{v}_e^2 + \hat{a}_e^2)(\hat{v}_f^2 + \hat{a}_f^2)}{(1 - M_Z^2/s)^2}\right] G_1 \\ &+ \frac{\hat{a}_e^2 + \hat{v}_e^2}{(1 - M_Z^2/s)^2}\left[\hat{a}_f^2\sum_{i=2}^{6} G_i + \hat{v}_f^2(G_4 + G_6)\right] + \frac{Q_eQ_f\hat{v}_e\hat{v}_f}{1 - M_Z^2/s}G_6\Bigg\}\end{aligned} \tag{7}$$

$x_{1,2} = 2E_{f,\bar f}/\sqrt{s}$ are the reduced energies of the fermions. [Later we shall use the variables $x_{12} = (1-x_1)(1-x_2)$ and $x = 2E_H/\sqrt{s} = 2 - x_1 - x_2$]. $\sigma_0 = 4\pi\alpha^2/3s$ is the standard normalization cross section. The coefficients G_1 and G_2 describe the Higgs radiation off the fermion f,

$$
\begin{aligned}
G_1 &= \frac{g_{ffH}^2}{4\pi}\frac{1}{x_{12}}\left[x^2 - h\left(\frac{x^2}{x_{12}} + 2(x-1-h)\right) + 2f\left(4(x-h) + \frac{x^2}{x_{12}}(4f-h+2)\right)\right] \quad (8)\\
G_2 &= -\frac{g_{ffH}^2}{4\pi}\frac{2}{x_{12}}\left[x_{12}(1+x) - h(x_{12}+8f+2x-2h) + 3fx\left(\frac{x}{3} + 4 + \frac{x}{x_{12}}(4f-h)\right)\right]
\end{aligned}
$$

with $f = m_f^2/s$, $h = M_H^2/s$ [and $z = M_Z^2/s$ to be used later on]. The coefficient G_1 agrees with the corresponding expression in Ref.[9] and in the limit of vanishing fermion and Higgs masses the clumsy Dalitz plot density reduces to the simple form [17]

$$
\begin{aligned}
\text{vector coupling} &\sim \frac{x^2}{(1-x_1)(1-x_2)}\\
\text{axial coupling} &\sim \frac{x^2}{(1-x_1)(1-x_2)} - 2(1+x)
\end{aligned}
$$

The remaining terms account for the emission of the Higgs particle from the Z–boson line (G_3, G_4), and the interference terms (G_5, G_6) between the radiation amplitudes off the fermion and the Z–boson lines

$$
\begin{aligned}
G_3 &= \frac{g_{ZZH}^2}{4\pi}\frac{2}{p^2}\left[f(4h - x^2 - 12z) + \frac{f}{z}(4h - x^2)(x-1-h+z)\right]\\
G_4 &= \frac{g_{ZZH}^2}{4\pi}\frac{2z}{p^2}\left[h + x_{12} + 2(1-x) + 4f\right]\\
G_5 &= -\frac{g_{ffH}g_{ZZH}}{4\pi}\frac{4xm_f/M_Z}{x_{12}p}\left[(x_{12}-h)(x-1-h) + f(12z - 4h + x^2) - 3z(h - \frac{2x_{12}}{x})\right]\\
G_6 &= -\frac{g_{ffH}g_{ZZH}}{4\pi}\frac{4zm_f/M_Z}{x_{12}p}\left[x(h-4f-2) - 2x_{12} + x^2\right] \quad (9)
\end{aligned}
$$

The denominator of the scaled propagator has been abbreviated by $p = x - 1 - h + z$.

It is well–known that the top quark production in e^+e^- annihilation, $e^+e^- \to t\bar t$, at very high energies is primarily mediated by photon exchange. Higgs radiation off the top quarks will therefore be the dominant mechanism so that the ttH Yukawa coupling can be measured directly through this process.

The integrated cross sections are shown for various values of the top mass in Fig.2a as a function of the Higgs mass. The total e^+e^- c.m. energy is chosen to be $\sqrt{s} = 500$ GeV. While for light Higgs masses the cross section increases with the top mass as a result of the rising Yukawa coupling, this trend is reversed for heavy Higgs particles by the reduction of the available phase space. With increasing total c.m. energy to 1 TeV, the cross sections decrease slightly for small Higgs masses, a consequence of scaling, while they fall off less steeply for large Higgs masses [Fig.2b]. It is demonstrated in Tab.1 that bremsstrahlung off the top quark is the dominant production process indeed. Only a small fraction of the cross section is due to Higgs emission from the Z–boson line [less than 6% in the entire range of Higgs and top masses that we have chosen]. For an energy of $\sqrt{s} = 500$ GeV and an integrated luminosity of $\int\mathcal{L} = 20$ fb^{-1}, corresponding to $\mathcal{L} = 2\times10^{-33}$ cm^{-2}s^{-1} and a run time of 10^7 s in a year, some 100 events can be expected at Higgs masses of order 60 GeV, falling to 20 events at 120 GeV. Taking acceptance losses into account [11], this appears to be the upper limit at which the ttH coupling can be directly measured in the intermediate mass range below the $t\bar t$ threshold in the course of a few years.

Since the signature of the process $e^+e^- \to t\bar tH$ is spectacular, see eq.(4), there is reasonable hope to isolate the events experimentally despite the low rates. The large number of b quarks in the final state $WWbbbb$ together with the mass constraints, $m(Wb) = m(t)$ for top and antitop and $m(b\bar b) = m(H)$ for the Higgs, will be crucial in rejecting background events. Even though simulations are needed that are based on detailed efficiencies for b tagging and W reconstruction, it can at least be shown that the background from QCD processes to $t\bar tb\bar b$ final states is small. A rough estimate of the total cross section $\sigma(e^+e^- \to t\bar tg^* \to b\bar bt\bar t)$ gives $\sigma < 3$ fb for $m_t > 120$ GeV. The additional requirement that the invariant mass of a $b\bar b$ pair coincides with the Higgs mass within the experimental resolution will reduce the background drastically [for instance if one just requires $m(b\bar b) \geq 50$ GeV, the background cross section decreases by a factor ~ 20]. The other process $e^+e^- \to b\bar bg^* \to t\bar tb\bar b$ is suppressed because the gluon must be highly virtual to generate a heavy $t\bar t$ pair. Another source of background for $M_H \sim M_Z$ will be the process $e^+e^- \to t\bar tZ$. The total cross section [8] is of the same size as $t\bar tH$ but drops by one order of magnitude if we require the Z boson to decay into $b\bar b$ pairs.

3 Minimal SUSY Extension

The minimal supersymmetric extension of the Standard Model generates a mass spectrum of Higgs particles that can be easily explored in e^+e^- colliders with a total energy of order 300 to 500 GeV. The model requires the existence of two doublets of scalar fields Φ_1 and Φ_2 with opposite hypercharge. The neutral component of the field Φ_2 (with vacuum expectation value v_2) couples only to up–type quarks while Φ_1 (with vacuum expectation value v_1) couples to down-type quarks and charged leptons. This extension of the Higgs sector introduces five physical Higgs particles: two $\mathcal{CP}$–even neutral bosons h^0 and H^0 (where h^0 will be taken as the lighter particle), a $\mathcal{CP}$–odd neutral boson A^0 (usually called pseudo–scalar) and two charged Higgs bosons $H^\pm$.

Besides the four masses of the physical states, two additional parameters define the properties of the scalar particles and their interactions with gauge bosons and fermions: the ratio of the two vacuum expectation values $\mathrm{tg}\beta = v_2/v_1$ and a mixing angle α in the neutral $\mathcal{CP}$–even sector. However, supersymmetry leads to several relations between these parameters and, in fact, only two of them are independent. These relations impose a strong hierarchical structure on the mass spectrum [$M_{h^0} < M_Z, M_{A^0} < M_{H^0}$ and $M_W < M_{H^\pm}$] which however is broken by radiative corrections if the top mass is large [18,19]. The parameter $\mathrm{tg}\beta$ will be assumed in the range $1 < \mathrm{tg}\beta < m_t/m_b$ [$\pi/4 < \beta < \pi/2$], consistent with GUT restrictions on the model.

An attractive choice of the two independent parameters is the set $(M_{h^0}, \mathrm{tg}\beta)$ from which all other masses and the angle α can be derived once the top quark mass and the associated squark masses are specified. The leading part of the radiative correction[1] is determined by the parameter ϵ which grows with the fourth power of the top quark mass m_t and logarithmically with the squark mass M_S [19],

$$\epsilon = \frac{3}{2}\frac{\alpha}{\pi}\frac{1}{s_W^2 c_W^2}\frac{1}{\sin^2\beta}\frac{m_t^4}{M_Z^2}\log\left(1+\frac{M_S^2}{m_t^2}\right) \tag{10}$$

These corrections are positive and they shift the mass of the lightest neutral Higgs boson upward with increasing top mass. The variation of the upper limit of M_{h^0} with the top quark mass is shown in Fig.3a for $M_S = 500$ GeV and three representative values of the ratio of vacuum expectation values $\mathrm{tg}\beta = 2.5$, 5 and 20.

Taking M_{h^0} and $\mathrm{tg}\beta$ as the base parameters, the mass of the pseudo–scalar state A^0 is given by

$$M_{A^0}^2 = \frac{M_{h^0}^2(M_Z^2 - M_{h^0}^2 + \epsilon) - \epsilon M_Z^2\cos^2\beta}{M_Z^2\cos^2 2\beta - M_{h^0}^2 + \epsilon\sin^2\beta} \tag{11}$$

and the masses of the heavy neutral and the charged Higgs boson follow from the sum rules [for $\mu = A_t = 0$]

$$M_{H^0}^2 = M_{A^0}^2 + M_Z^2 - M_{h^0}^2 + \epsilon \tag{12}$$

$$M_{H^\pm}^2 = M_{A^0}^2 + M_W^2 \tag{13}$$

For the three representative values of $\mathrm{tg}\beta$ introduced above, the masses M_{A^0}, M_{H^0} and $M_{H^\pm}$ are depicted in Fig.3b–3d, as a function of the light neutral Higgs mass M_{h^0}.

[1] For the sake of simplicity we shall neglect possible non-leading effects due to non-zero values of the supersymmetric Higgs–boson mass term μ and of the coefficient A_t of the soft–breaking term proportional to the superpotential. For a general discussion see [18].

Apart from the range near the upper limit of M_{h^0} for fixed $\mathrm{tg}\beta$ the mass values cluster in characteristic bands of 100 to 150 GeV for M_{H^0} and $M_{H^\pm}$, and up to ~ 100 GeV for M_{A^0} [similarly to M_{h^0}].

The mixing angle α is related to β and the Higgs masses by

$$\tan 2\alpha = \frac{(M_{A^0}^2 + M_Z^2)\sin 2\beta}{(M_{A^0}^2 - M_Z^2)\cos 2\beta + \epsilon} \qquad \left[-\frac{\pi}{2} < \alpha < 0\right] \tag{14}$$

The couplings of the various neutral Higgs bosons to fermions and gauge bosons will in general depend on the angles α and β. Normalized to the $\mathcal{SM}$ Higgs couplings, they are summarized in Table 2. Note that the couplings to down–type particles are strongly enhanced if $\mathrm{tg}\beta$ becomes large. Typical numerical values of the couplings which involve the mixing angle α are shown in Fig.4. There is in general a strong dependence on $\mathrm{tg}\beta$ and M_{h^0} which are taken as the input parameters.

The additional mechanism $e^+e^- \to A^0H^i \to t\bar{t}H^i$ for $H^i = h^0, H^0$ renders the amplitude in the $\mathcal{MSSM}$ more complicated than in the Standard Model. Using the same notation as in eq.(7) we find for the Dalitz plot density of the process $e^+e^- \to f\bar{f}H^i$

$$\begin{aligned}\frac{d\sigma(e^+e^-\to f\bar{f}H^i)}{dx_1dx_2} = N_c\frac{\sigma_0}{4\pi}\Bigg\{&\left[Q_e^2Q_f^2 + \frac{2Q_eQ_f\hat{v}_e\hat{v}_f}{1-M_Z^2/s} + \frac{(\hat{v}_e^2+\hat{a}_e^2)(\hat{v}_f^2+\hat{a}_f^2)}{(1-M_Z^2/s)^2}\right]G_1 \\ &+\frac{\hat{a}_e^2+\hat{v}_e^2}{(1-M_Z^2/s)^2}\left[\hat{a}_f^2\sum_{i=2}^{6}G_i + \hat{v}_f^2(G_4+G_6) + \frac{G_7}{16c_W^2s_W^2}\right] + \frac{Q_eQ_f\hat{v}_e\hat{v}_f}{1-M_Z^2/s}G_6\Bigg\}\end{aligned} \tag{15}$$

where all the functions G_k (k =1,..,6) are the same as in eqs.(8,9) apart from the change of the Yukawa couplings which are modified by the factors listed in Table 2. The additional diagram involving the pseudo–scalar boson A^0 is described by G_7 with

$$\begin{aligned}G_7 \;=\; &\frac{1}{4\pi}\frac{2g_{ffA}k_i}{x-1-h_i+h_A}\Bigg\{(4h_i - x^2)\left[k_ig_{ffA}\frac{x-1-h_i}{x-1-h_i+h_A} + \frac{2m_f}{M_Z}a_fg_{ZZH^i}\right] \\ &-2a_fg_{ffH^i}\frac{x}{x_{12}}\left[(x_{12}-h_i)(x-1-h_i) - f(4h_i - x^2)\right]\Bigg\}\end{aligned} \tag{16}$$

where $h_1 = M_{H^0}^2/s, h_2 = M_{h^0}^2/s, h_A = M_{A^0}^2/s$ and $a_f = 2I_{3L}^f$. The dimensionless factor k_i measures the strength of the coupling ZA^0H^i relative to the ZZH coupling; it is given in the last column of Table 2.

The production of the $\mathcal{CP}$–odd Higgs boson A^0 in association with a fermion pair does not involve Higgs emission from the Z–line. The Dalitz plot density is given in this case by

$$
\begin{aligned}
\frac{d\sigma(e^+e^- \to f\bar{f}A^0)}{dx_1 dx_2} &= N_c \frac{\sigma_0}{4\pi}\left\{\left[Q_e^2 Q_f^2 + 2\frac{Q_e Q_f \hat{v}_e \hat{v}_f}{1-M_Z^2/s} + \frac{(\hat{v}_e^2+\hat{a}_e^2)(\hat{v}_f^2+\hat{a}_f^2)}{(1-M_Z^2/s)^2}\right] F_1 \right. \\
&\left. + \frac{\hat{a}_e^2+\hat{v}_e^2}{(1-M_Z^2/s)^2}\frac{1}{16c_W^2 s_W^2}\left[a_f^2 F_2 + F_3 + a_f F_4\right]\right\} \qquad (17)
\end{aligned}
$$

where using the same notations as before,

$$
\begin{aligned}
F_1 &= \frac{g_{ffA}^2}{4\pi}\frac{1}{x_{12}}\left[x^2 - h_A\left(\frac{x^2}{x_{12}}(1+2f) + 2(x-1-h_A)\right)\right] \\
F_2 &= \frac{g_{ffA}^2}{4\pi}\frac{1}{x_{12}}\left[2(2h_A - x_{12})(1+x-h_A) - 4h_A(1+2f) - 2f\frac{x^2}{x_{12}}(x_{12}-3h_A)\right] \\
F_3 &= \frac{1}{4\pi}\left[\sum_i \frac{g_{ffA}k_i}{x-1-h_A+h_i}\right]^2 \times \frac{1}{2}(x-1-h_A+4f)(4h_A - x^2) \qquad (18) \\
F_4 &= -\frac{1}{4\pi}\sum_i\left[\frac{g_{ffA}g_{ffH^i}k_i}{x-1-h_A+h_i}\right] \times 2\frac{x}{x_{12}}\left[(x_{12}-h_A)(1-x+h_A) + f(4h_A - x^2)\right]
\end{aligned}
$$

The cross sections for $e^+e^- \to t\bar{t}h^0, t\bar{t}H^0$ and $f\bar{f}A^0$ at $\sqrt{s} = 500$ GeV are shown in Fig.5. Because the couplings are reduced by mixing angles in comparison to the $\mathcal{SM}$ couplings, the individual cross sections are correspondingly smaller. It will therefore be more difficult to detect $t\bar{t}H^i$ final states in the $\mathcal{MSSM}$ than in the $\mathcal{SM}$. The light neutral $\mathcal{CP}$–even Higgs boson h^0 could be accessible for small masses and small values of tgβ, and else large masses and large values of tgβ. The heavy $\mathcal{CP}$–even Higgs boson H^0 would be accessible in the mass range between 100 and 120 GeV. The cross section for the $t\bar{t}A^0$ final state is very small for values of tgβ larger than unity. In Fig.5b we show the cross sections for $e^+e^- \to f\bar{f}A^0$ [for b and τ final states we took into account only the bremsstrahl process]. In the case where the ZA^0H^i couplings are small, the bremsstrahlung off fermion lines provides in principle access to the pseudo–scalar boson in the processes $e^+e^- \to b\bar{b}A^0$ and $\tau^+\tau^-A^0$. However, the cross sections for these channels are sufficiently large only for large values of tgβ.

For the sake of completeness we have also studied the bremsstrahlung of charged Higgs bosons $e^+e^- \to t\bar{b}H^-$ and $\bar{t}bH^+$. This process is only of interest in the mass range where neither t can decay into H^+ nor H^+ into t. This leaves us with the small mass window $m_t - m_b < M_{H^\pm} < m_t + m_b$. Since the analytic expression of the Dalitz plot density is more complicated due to the presence of both top and bottom couplings and due to the different t and b masses, it will not be given here. The cross section, shown in Fig.5c, is sizeable only for extreme values of tgβ.

4 Conclusions

The measurement of the Higgs couplings to other fundamental particles provides one of the crucial tests of the Higgs mechanism. However it proves quite difficult to measure the Higgs couplings to fermions directly. A promising and nearly unique method, though experimentally not easy, is provided by Higgs bremsstrahlung off heavy top quarks in high–energy e^+e^- colliders. We have discussed this process in detail. Within the Standard Model the mass region up to $M_H \sim 120$ GeV can be explored in a collider of ~ 500 GeV c.m. energy. In the minimal SUSY extension of the Standard Model the cross sections are in general smaller unless the value of the parameter tgβ is either exceptionally large or small. For Higgs masses above the top threshold the measurement of the branching ratio for Higgs decays to top quarks opens a complementary mass range to measure the Higgs–top quark coupling.

References

[1] P. W. Higgs, Phys. Lett. 12 (1964) 132;
F. Englert and R. Brout, Phys. Rev. Lett. 13 (1964) 321;
G. S. Guralnik, C. R. Hagen and T. W. Kibble, Phys. Rev. Lett. 13 (1964) 585.

[2] S. Glashow, Nucl. Phys. B422 (1961) 579;
A. Salam, in Elementary Particle Theory, ed. N. Svartholm, (1968) 367;
S. Weinberg, Phys. Rev. Lett. 419 (1967) 1264.

[3] Ch. Llewellyn Smith, Phys. Lett. 46B (1973) 233;
J. S. Bell, Nucl. Phys. B60 (1973) 427;
J. M. Conrnwall, D. N. Levine and G. Tiktopoulos, Phys. Rev. Lett. 30 (1973) 1268.

[4] J. Ellis, M.K. Gaillard and D.V. Nanopoulos, Nucl. Phys. B106 (1976) 292;
J.D. Bjorken, Proc. SLAC Summer Institute, 1976;
B. Ioffe and V. Khoze, Sov. J. Part. Nucl. Phys. 9 (1978) 50;
B.W. Lee, C. Quigg and H.B. Thacker, Phys. Rev. D16 (1977) 1519.

[5] D.R.T. Jones and S.T. Petcov, Phys. Lett. 84B (1979) 440;
R.N. Cahn and S. Dawson, Phys. Lett. 136B (1984) 196.
G. Altarelli, B. Mele and Pitolli, Nucl. Phys. B287 (1987) 205.

[6] R. Kleiss, Z. Kunszt and J. W. Stirling, Phys. Lett. 253B (1991) 269.

[7] L. Resnick, M.K. Sundaresan and P.J.S. Watson, Phys. Rev. D8 (1973) 172;
F. Wilczek, Phys. Rev. Lett. 39 (1977) 1304;
J. Ellis, M.K. Gaillard and D.V. Nanopoulos, Nucl. Phys. B106 (1976) 292;
H.M. Georgi, S.L. Glashow, M.E. Machacek and D.V. Nanopoulos, Phys. Rev. Lett. 40 (1978) 692;
A. Djouadi, M. Spira, J. van der Bij and P. M. Zerwas, Phys. Lett. 257B (1991) 187;
A. Djouadi, M. Spira and P. M. Zerwas, Phys. Lett. 264B (1991) 440.

[8] K. Hagiwara, H. Murayama and I. Watanabe, KEK preprint TH–264 (1990).

[9] K.J.F. Gaemers and G.J. Gounaris, Phys. Lett. 77B (1978) 379.

[10] Z. Kunszt, Nucl. Phys. B247 (1984) 339;
J. F. Gunion, Phys. Lett. 261B (1991) 510;
Z. Kunszt, Z. Trocsanyi and W. J. Stirling, ETH Zurich Preprint, ETH–TH–91–17.

[11] B. Wiik, Workshop on Physics and Experiments with Linear Cooliders, Saariselkä (Finland), Sept. 1991.

[12] J. Kalinowski and S. Pokorski, Phys. Lett. 219B (1989) 116;
J. Kalinowski, preprint TUM-T31-14/91, to appear in Proc. XIV Warsaw Symposium on Elementary Particle Physics, May 1991.

[13] A. Bartl, W. Majerotto and N. Oshimo, Phys. Lett. 237B (1990) 229;
J. Kalinowski and H.-P. Nilles, Phys. Lett. 255B (1991) 134.

[14] A. Djouadi, P.M. Zerwas and J. Zunft, Phys. Lett.259 (1991) 175.

[15] H. Baer and X. Tata, Phys. Lett. 167B (1986) 241;
L.A.T. Bauerdick, Z. Phys. C32 (1986) 459;
T. G. Rizzo, Preprint MAD–PH–649 (1991).

[16] J. Gunion, H. Haber, G. Kane and S. Dawson, The Higgs Hunter's Guide, Addison–Wesley, Reading, MA, 1990.

[17] E. Laermann, K. H. Streng and P. Zerwas, Z. Phys. C3 (1979) 289 and erratum.

[18] Y. Okada, M. Yamaguchi and T. Yanagida, Prog. Theor. Phys. 85 (1991) 1;
H. Haber and R. Hempfling, Phys. Rev. Lett. 66 (1991) 1815;
J. Ellis, G. Ridolfi and F. Zwirner, Phys. Lett. 257B (1991) 83 and CERN–TH–6002/91;
R. Barbieri, F. Caravaglios and M. Frigeni, Phys. Lett. 258B (1991) 167.

[19] R. Barbieri and M. Frigeni, Phys. Lett. 258B (1991) 395.

FIGURE CAPTIONS

Fig.1. (a) Generic diagrams for Higgs bremsstrahlung $e^+e^- \rightarrow t\bar{t}H$ in the Standard Model $\mathcal{SM}$; (b),(c) production of neutral Higgs bosons in $f\bar{f}h^0$, $f\bar{f}H^0$ and $f\bar{f}A^0$ final states, (d) charged Higgs bosons $H^\pm$ in $t\bar{b}H^-$ final states within two-Higgs doublet models.

Fig.2. The cross section $\sigma(e^+e^- \rightarrow t\bar{t}H)$ in the Standard Model as a function of the Higgs mass for three representative values of the top mass, $m_t = 120, 150$ and 180 GeV; (a) total c.m. energy $\sqrt{s} = 500$ GeV, (b) $\sqrt{s} = 1$ TeV.

Fig.3. The masses of the Higgs particles in the minimal SUSY extension of the Standard Model $\mathcal{MSSM}$ including radiative corrections; the squark mass is fixed to $M_S = 500$ GeV. (a) Upper mass limit of the lightest scalar h^0 as a function of the top quark mass; (b)-(d) masses of H^0, A^0 and $H^\pm$ as a function of the h^0 mass, m_t fixed to 130 GeV.

Fig.4. Coupling parameters of SUSY Higgs bosons in relation to $\mathcal{SM}$ couplings as defined in Table 2. [For a given tgβ the curves terminate at the upper limit of M_{h^0}.]

Fig.5. Production cross sections for SUSY Higgs bosons in association with heavy quarks and τ leptons; (a) neutral scalar Higgs bosons h^0 and H^0; (b) pseudo-scalar Higgs A^0; (c) charged Higgs $H^\pm$.

M_H / m_t	120	150	180
60	0.96	0.98	0.99
90	0.95	0.98	0.99
120	0.94	0.98	0.99

Table 1: Fraction of the cross section for Higgs radiation off the fermion line without radiation off the $Z-$ boson line for a set of typical top and Higgs mass values [in GeV].

	$u\bar{u}$	$d\bar{d}$	ZZ	ZA^0H^i
H	1	1	1	–
h^0	$\cos\alpha/\sin\beta$	$-\sin\alpha/\cos\beta$	$\sin(\beta-\alpha)$	$\cos(\beta-\alpha)$
H^0	$\sin\alpha/\sin\beta$	$\cos\alpha/\cos\beta$	$\cos(\beta-\alpha)$	$-\sin(\beta-\alpha)$
A^0	$1/\tan\beta$	$\tan\beta$	0	–

Table 2: Higgs couplings in the minimal SUSY extension of the Standard Model to fermion and gauge boson pairs, relative to the $\mathcal{SM}$ couplings. For the last column the couplings are given in units of the ZZH coupling in the $\mathcal{SM}$.

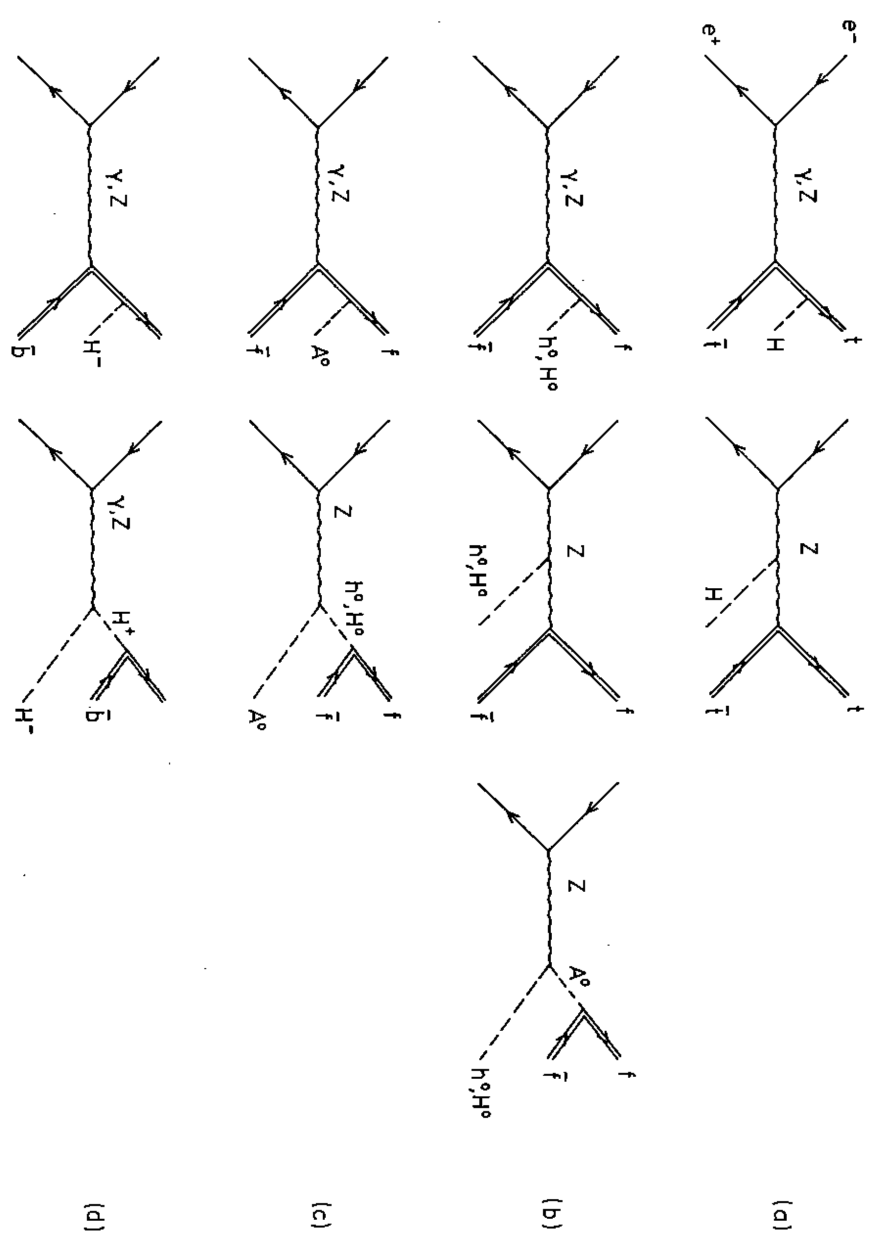

e⁻
e⁺
γ,Z
Z
t
H
t̄
f
f̄
h°,H°
A°
H⁻
H⁺
b̄
(a)
(b)
(c)
(d)

Fig. 1

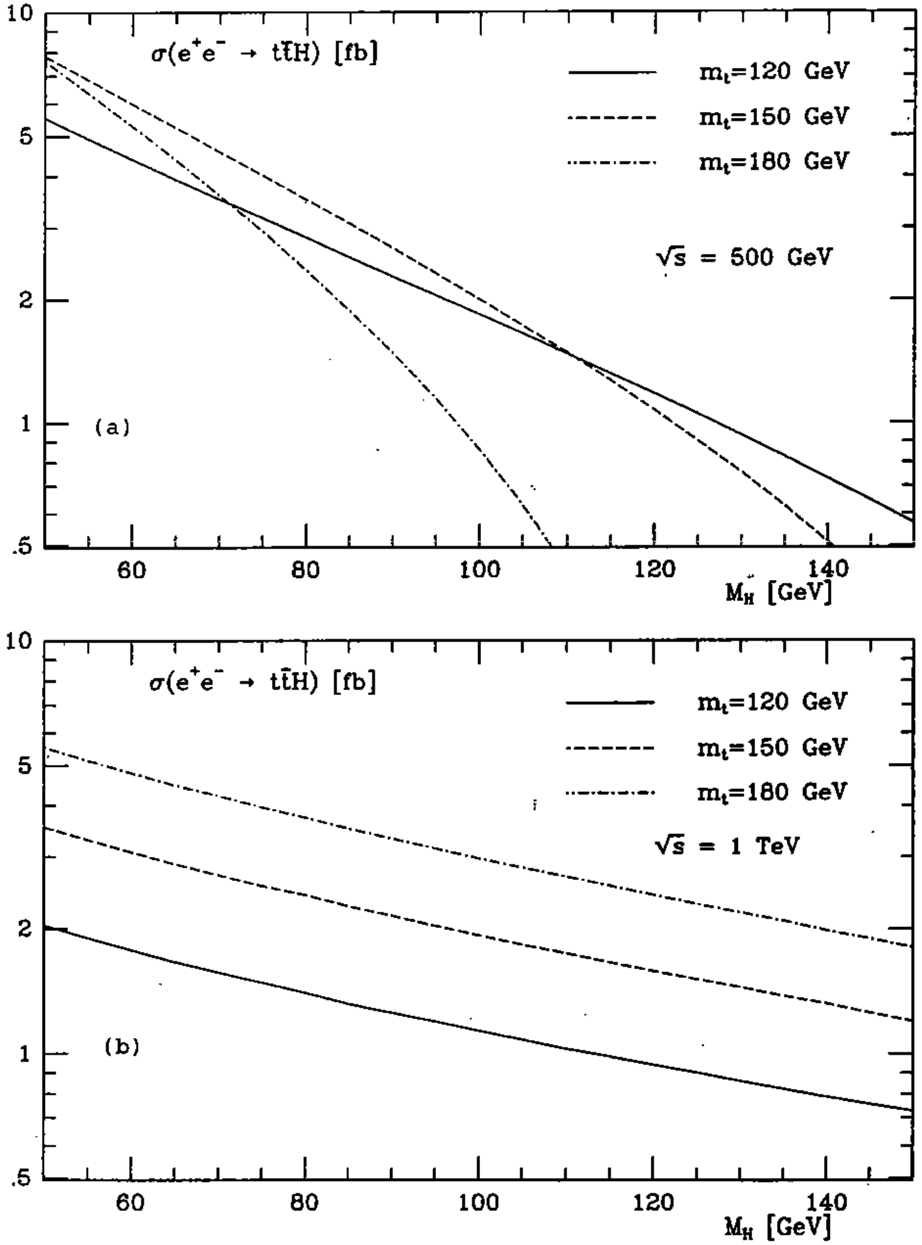

$\sigma(e^+e^- \to t\bar{t}H)$ [fb]
m_t=120 GeV
m_t=150 GeV
m_t=180 GeV
$\sqrt{s}$ = 500 GeV
(a)
$\sqrt{s}$ = 1 TeV
(b)
M_H [GeV]

Fig. 2

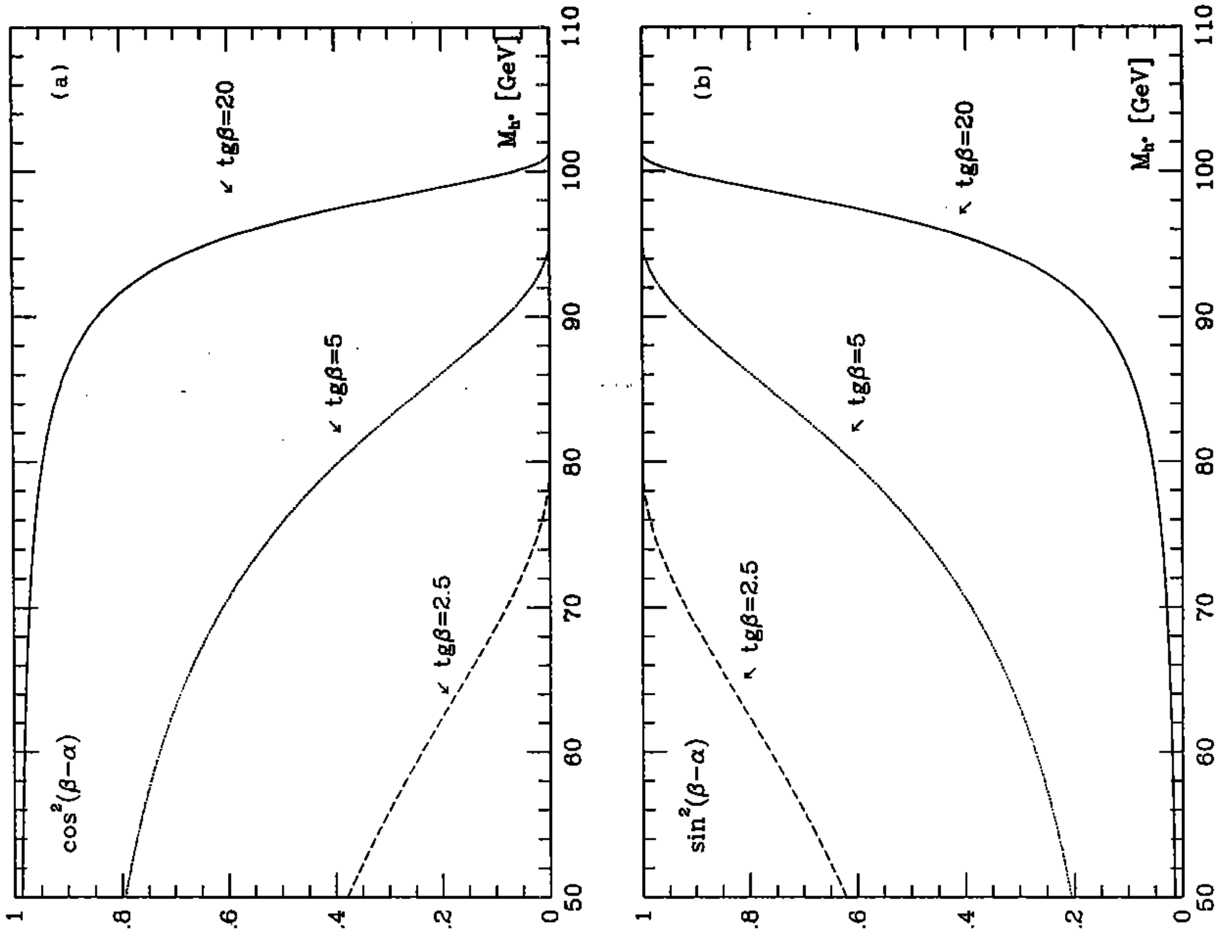

(a)
$\cos^2(\beta-\alpha)$
tgβ=20
tgβ=5
tgβ=2.5
M_{h^0} [GeV]
(b)
$\sin^2(\beta-\alpha)$
tgβ=20
tgβ=5
tgβ=2.5
M_{h^0} [GeV]

Fig. 4

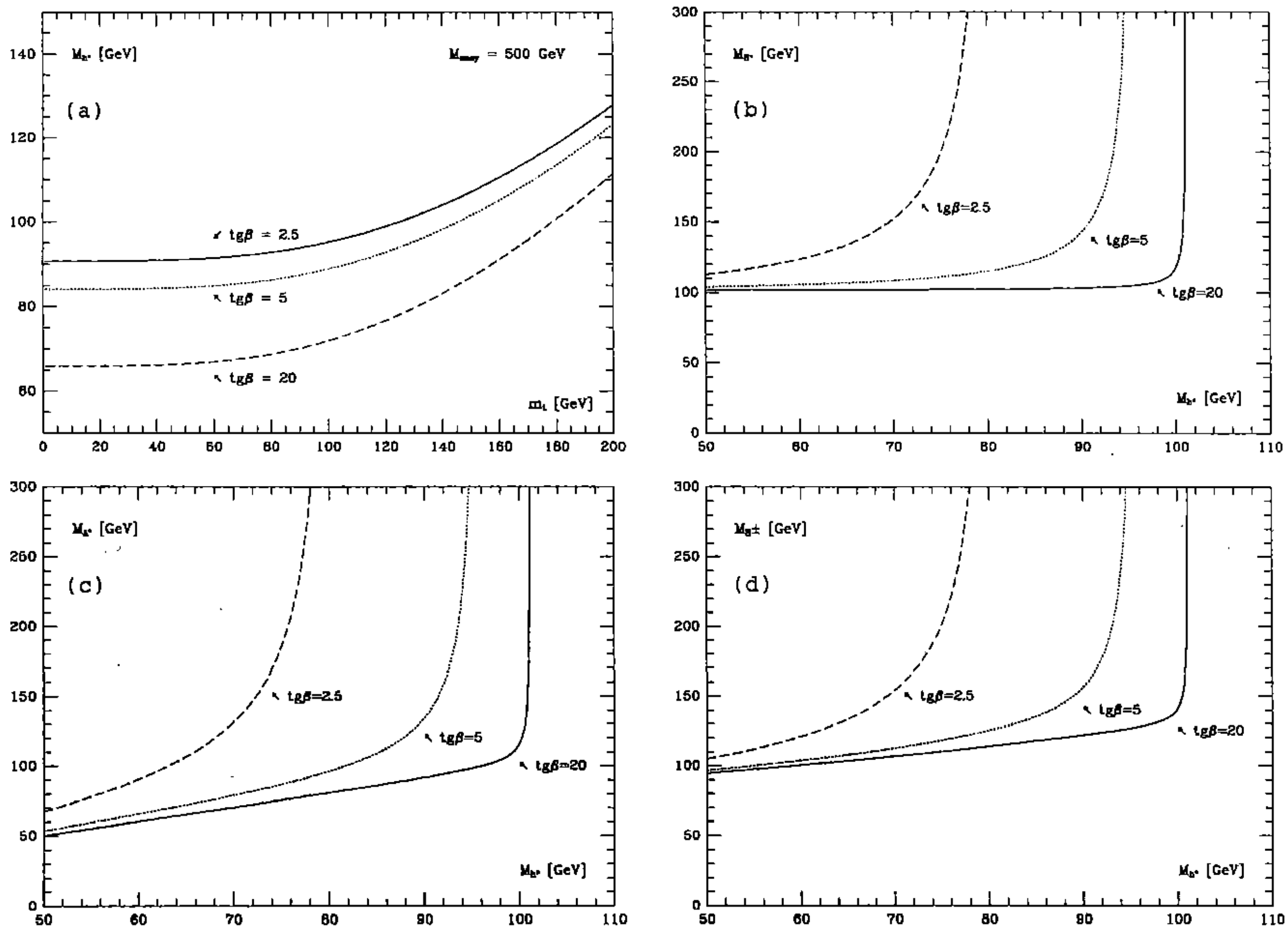

M_{h^0} [GeV]
M_{susy} = 500 GeV
(a)
tgβ = 2.5
tgβ = 5
tgβ = 20
m_t [GeV]
M_{H^0} [GeV]
(b)
tgβ=2.5
tgβ=5
tgβ=20
M_{h^0} [GeV]
M_{A^0} [GeV]
(c)
tgβ=2.5
tgβ=5
tgβ=20
M_{h^0} [GeV]
$M_{H^\pm}$ [GeV]
(d)
tgβ=2.5
tgβ=5
tgβ=20
M_{h^0} [GeV]

Fig. 3

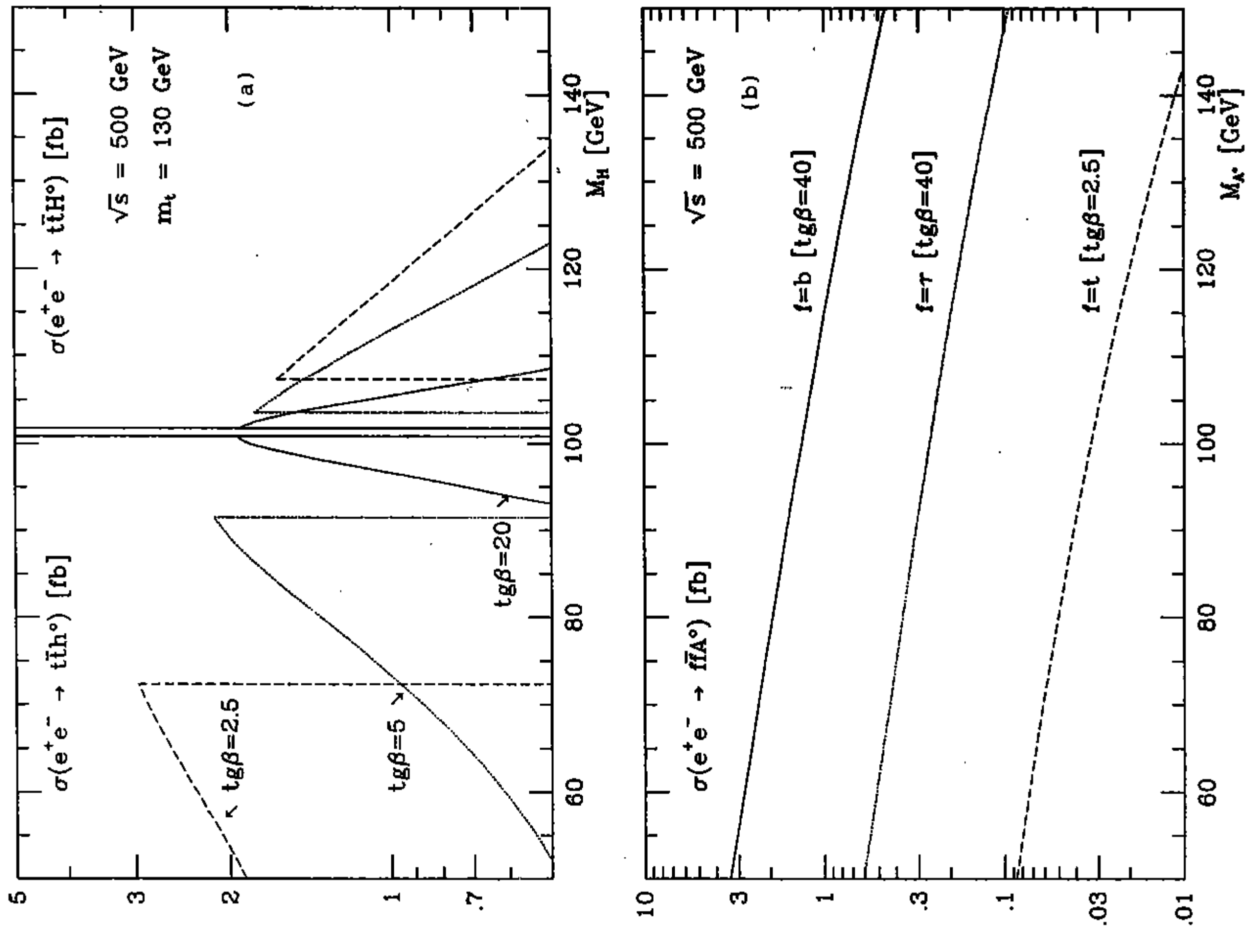

Fig. 5

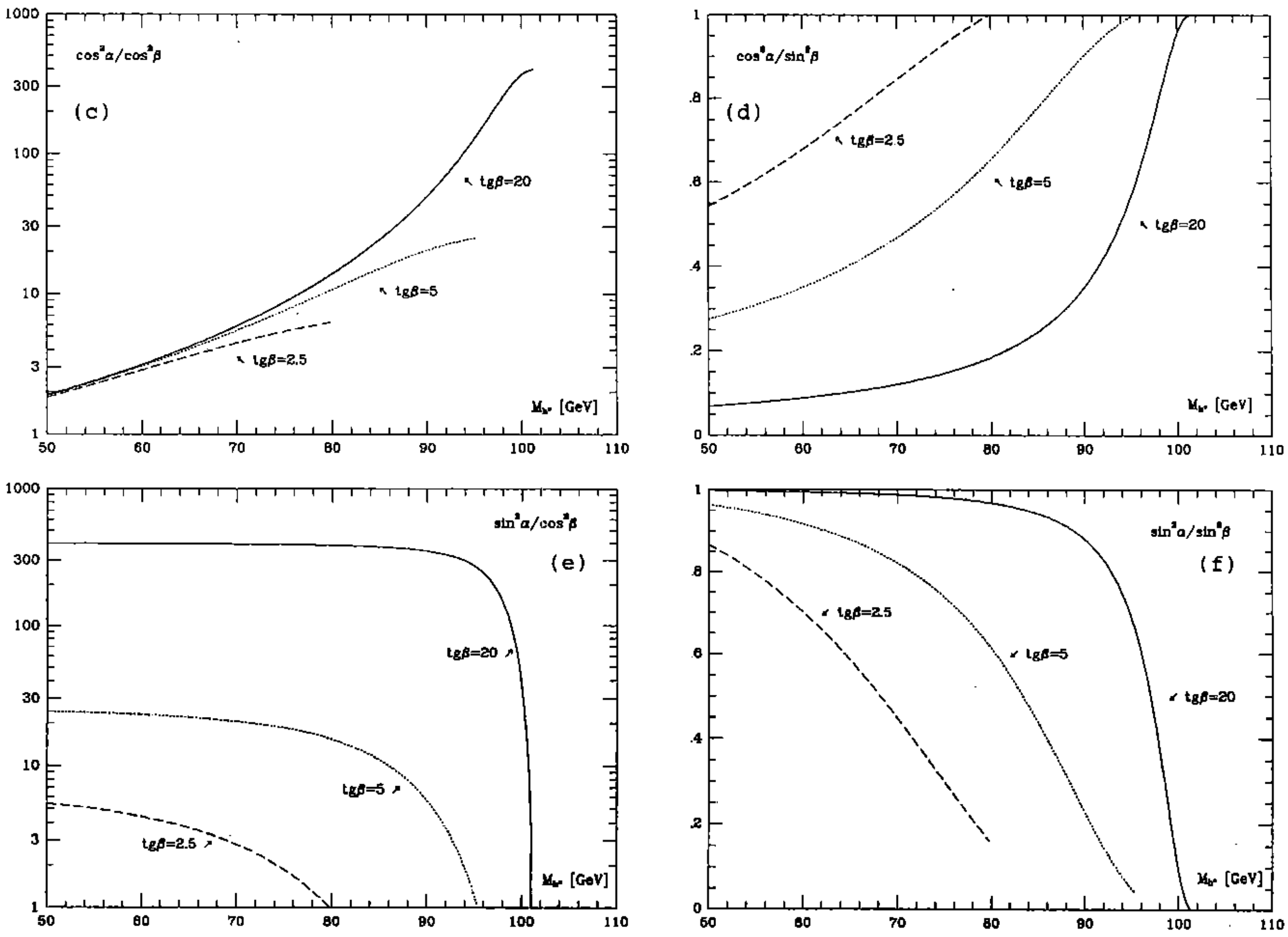

Fig. 4, cont'd

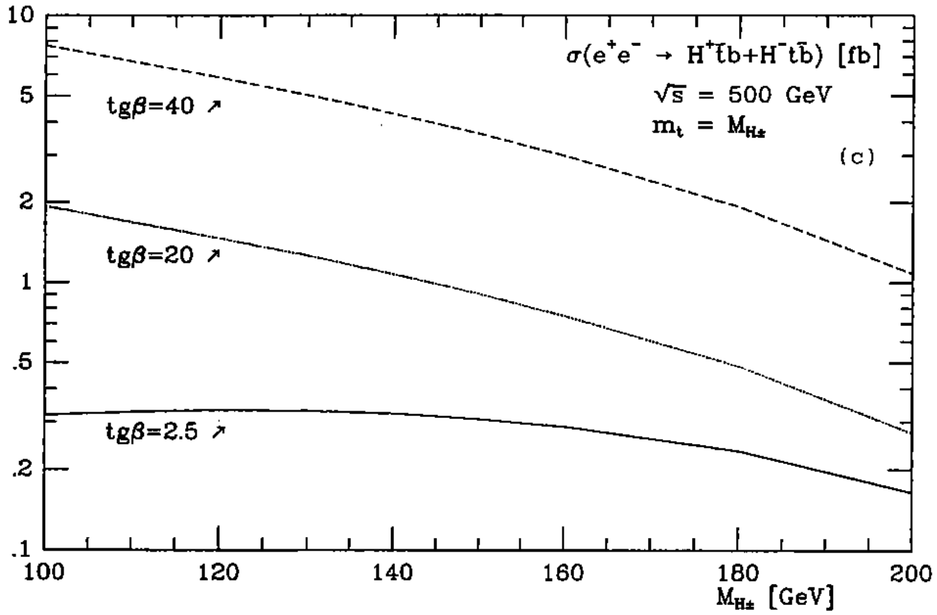
$\sigma(e^+e^- \to H^+\bar{t}b+H^-t\bar{b})$ [fb]
$\sqrt{s}$ = 500 GeV
$m_t = M_{H\pm}$
(c)
tgβ=40
tgβ=20
tgβ=2.5
10
5
2
1
.5
.2
.1
100
120
140
160
180
200
$M_{H\pm}$ [GeV]

Fig. 5 cont'd